

New Method to Distinguish Adhesion and Cohesion Stresses in Metal/Polymer Composites

Marcos Vinicius Utumi^a , Leandro Luís Corso^b , Alexandre Luís Gasparin^{a,*} 

^aInstituto Federal de Educação Ciência e Tecnologia do Rio Grande do Sul, Programa de Pós-Graduação em Tecnologia e Engenharia de Materiais (PPGTEM), R. Avelino Antônio de Souza, 1730, 95043-700, Nossa Senhora de Fátima, RS, Brasil

^bUniversidade de Caxias do Sul, Caxias do Sul, RS, Brasil

Received: June 24, 2020; Revised: December 09, 2020; Accepted: December 27, 2020

This study aims at presenting a new analysis method for adhesive (interfacial) and cohesive (bulk) failures in aluminum (Al) and high-density polyethylene (HDPE) sandwich composites. The samples were submitted to tensile strength tests, according to ASTM C297 so as to obtain the pull-off stresses. The delaminated aluminum surfaces were analyzed with SEM/EDS (Scanning Electronic Microscopy with Energy Dispersive Scanning). The images were calculated using a genetic algorithm (GA), where the areas with cohesive and adhesive failures were identified by the presence or absence of organic compounds. The proposed method also uses the data from the pull-off tests to determine the stress values of adhesion and cohesion separately. Applying the new method, the mean stress of cohesion was 4.17 MPa, and for adhesion it was 0.57 MPa. Thus, it was possible to distinguish and calculate the failure stresses applied to metal/polymer composites.

Keywords: sandwich composite, adhesion and cohesion strength, genetic algorithm.

1. Introduction

The manufacturing process of an aluminum and polyethylene composite is used in several areas, from the food industry packaging to construction and auto industry revetments^{1,2}. However, adhesion between materials remains a challenge when the surfaces that are not treated delaminate easily². Currently, polymer matrix composites have attracted the interest of researchers and industries because the combination of those materials present better properties than those obtained with the materials used individually³. Also, natural fillers are an option extensively applied for the natural fiber-reinforced composites in the packaging industry as excellent mechanical supports with functional electrical and bio-material features^{4,6}.

The improvement in HDPE adhesion properties can be achieved through a series of surface treatments prior to the occurrence of the surfaces adhesion⁷. It is also important to register that the modification of surfaces and loads used for a composite can be adjusted with the results of adhesion properties, thus developing a more adequate material for the application⁸.

Considering adhesion as the interaction between surfaces, it can be studied microscopically or macroscopically. The intermolecular interactions depend mainly on the interface, while macroscopically it is characterized by the work necessary to separate the adhering sides⁹. The composite material interface surfaces may or may not need a developer for that interaction. The adhesion is considered direct when it occurs without a third layer on the interface, and indirect when there is a glue or tape on the surface of each sheet promoting the adhesion to the composite material. In the attempt to pull off this area, two types of failures might occur. One is the

cohesive failure, or the internal (bulk) rupture of one of the components; the other is the adhesive failure, occurring on the interface of the adhered materials¹⁰.

The adhesive/cohesive failure, being a phenomenon that occurs between two surfaces, is generally categorized as adhesive when the separate materials are different, and cohesive when the adhering surfaces are of the same material. In some situations, adhesion and cohesion may occur simultaneously¹¹. Figure 1 represents a failure that occurs in a sandwich composite after a destructive test. In the last frame, presented in Figure 1, it is possible to observe the occurrence of both failures. The main purpose of this study is to quantify how much adhesive and cohesive stress there is in that situation.

The main problem in determining the adhesion stress is that the metal-polymer interface has two types of failures, which means that the stress to separate the materials is due to the interface delamination and to the cohesion of one of the composite parts only¹². There are several tests to determine the adhesion stress, but most of them do not quantify or discriminate each of the failures, adhesion or cohesion, for obtaining information on the interface strength of the composite material^{13,14}.

In a composite material where there is 100% cohesive failure it becomes clear that the maximum adhesion stress in the interface is higher than the cohesion stress. However, how to have the dimensions or how to plan for a composite material in which both adhesive and cohesive interface failures occur? This kind of material could have a different approach, once the interface mechanical properties are known. One solution this study offers is by determining the maximum adhesion and cohesion stress separately by using the pull-off test results, SEM images and EDS chemical

*e-mail: alexandre.gasparin@caxias.ifs.edu.br.

composition analyses to distinguish the respective stress areas, applying a genetic algorithm with a convergence criterion to characterize properly such failure.

This study presents the application of a technique to understand the adhesion phenomenon using surface analysis. Considering the adhesion between two materials as fundamental for the application in a sandwich composite, it was possible to correlate the surface composition of Al/HDPE interlaminar failure to the different form of rupture in the pull-off test: polymer adhered to the metal sheet (bulk) or naked metal (interfacial) after testing. Once, the aluminum sheet won't rupture by the adhesion of the polyethylene, the absence of carbon on aluminum surface after testing provides the adhesion area, nevertheless, the presence of carbon indicates the polymer bulk rupture or the cohesion area.

2. Material and Methods

2.1 Characterization of materials

The sandwich composite was hot pressed with the following parameters: 350 °C heated aluminum sheet, 150 N compressive force for 2 minutes, and manufactured with two layers (Al/HDPE). All sheets had the same contact area (25x25 mm²), but the HDPE thickness was 5.0 mm, while the aluminum 1.2 mm. The contact surfaces were clean with alcohol isopropyl before pressing.

Fourier-transform infrared spectroscopy (FTIR) was performed in the equipment PerkinElmer FT-IT Frontier to characterize the HDPE, which presented a PE probability of 98%. The HDPE was obtained with a density of 0.96 g/cm³. The aluminum sheet underwent a SEM/EDS test, with a TESCAN MIRA 3 equipment. A composition of aluminum sheets AA3105H16 was obtained, as specified by the supplier.

2.2 Experimental procedure

The research applied to investigate and validate the methodology was performed according to the sequence presented in Figure 2.

In the phase of surface analysis through SEM/EDS, the images obtained were processed with the use of Matlab[®] software. The application developed used the Equations 1, 2, and 3 to calculate the relation between the image generated and the composition given by the equipment, determining an area containing a particular chemical composition (energy in the carbon range).

$$\%E_X(\text{tescan}) = \%E_X(\text{im_eval}) \quad (1)$$

$$\%E_{X(\text{im_eval})} = \sum_{i=j}^n [X_{11} \dots X_{nn}]_r \cup \sum_{i=j}^n [X_{11} \dots X_{nn}]_g \cup \sum_{i=j}^n [X_{11} \dots X_{nn}]_b \quad (2)$$

$$[X_{11} \dots X_{nn}]_{rgb} = [X_{11} \dots X_{nn}]_r + [X_{11} \dots X_{nn}]_g + [X_{11} \dots X_{nn}]_b \quad (3)$$

Equation 1 represents a comparison between the figures obtained by the equipment and the image analysis, where “%E_X(tescan)” represents the chemical composition or the element “X” ratio, while “%E_X(im_eval)” represents the composition obtained through the analysis of the application. The image evaluation equals the sum of the individual matrices for each primary color having a higher result to factor “r_x”, “g_x” or “b_x” (colors red, green and blue, respectively, in quantities in the SEM/EDS image) and calculated according to the reference value. The individual matrices are the result of Equation 3, where the image is divided in three matrices, one for each corresponding primary color. In a simplified way, the calculation method developed by Matlab[®] will count the pixels in the image, correlating the value of its chemical composition to determine the position and distribution of the material represented in the matrix.

Figure 3 presents the application developed in Matlab[®], named Adhesive Surface Image Processing (ASIP). First, an image of the chemical composition of each element is formed by the EDS data shown in Figure 3a. The table in Figure 3b shows the chemical composition (EDS), and the area (ASIP) of each element, and the unit is the sum of ASIP

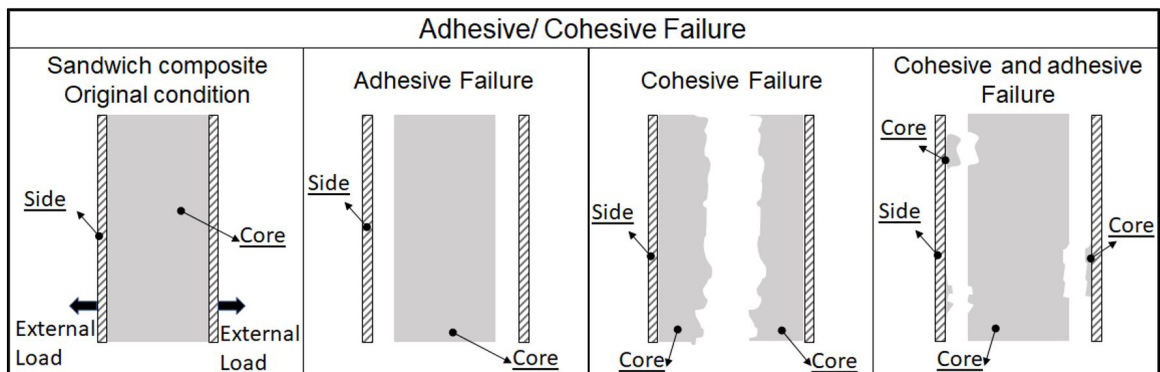


Figure 1. Adhesive/cohesive failure.



Figure 2. Sequence of the work phases.

column values. The column EDS of Figure 3c sums 1.0137, a residual value of .0137 (approximately 1.4%) is considered part of the EDS error. The SEM IMAGE shown in Figure 3c is the original image processed from the microscope.

The samples were tested according to the tensile strength pull-off test ASTM C297¹⁵, which determines the flatwise tensile strength of the core, the core-to-facing bond, or the facing of an assembled sandwich composite. Figure 4 shows a diagram of how samples are adhered in bonding blocks with high strength epoxy adhesive, the interfacial fracture, and the HDPE adhered residues over the aluminum surface. The testing method consists on the controlled application of a normal uniaxial stress to the external surface of each composite sheet until the delamination or rupture in the interface of the composite material occurs. Resistance to the maximum tensile strength is calculated as per Equation 4. The SEM images and EDS data are generated after testing, as indicates the Figure 4.

$$\sigma_z^{ftu} = \frac{P_{max}}{A} \tag{4}$$

Where " σ_z^{ftu} " is the ultimate flatwise tensile strength, " P_{max} " is the maximum load and " A " is the section area¹⁶.

A second routine estimates the areas of adhesive and cohesive failures according to carbon distribution on the surface as per Equations 5 and 6.

$$Im_{size} = Adh_{failure} + Coh_{failure} \tag{5}$$

$$Coh_{failure} = \frac{\sum_{i=1}^n j^i = C_{rgb} [C_{11} \dots C_{nn}]_{rgb}}{nxn} \tag{6}$$

Where " Im_{size} " equals the full matrix, " $Adh_{failure}$ " is the part of the matrix presenting the adhesive failure and " $Coh_{failure}$ " is the area showing the cohesive failure. The failures are calculated according to the sum of the cells containing energy values

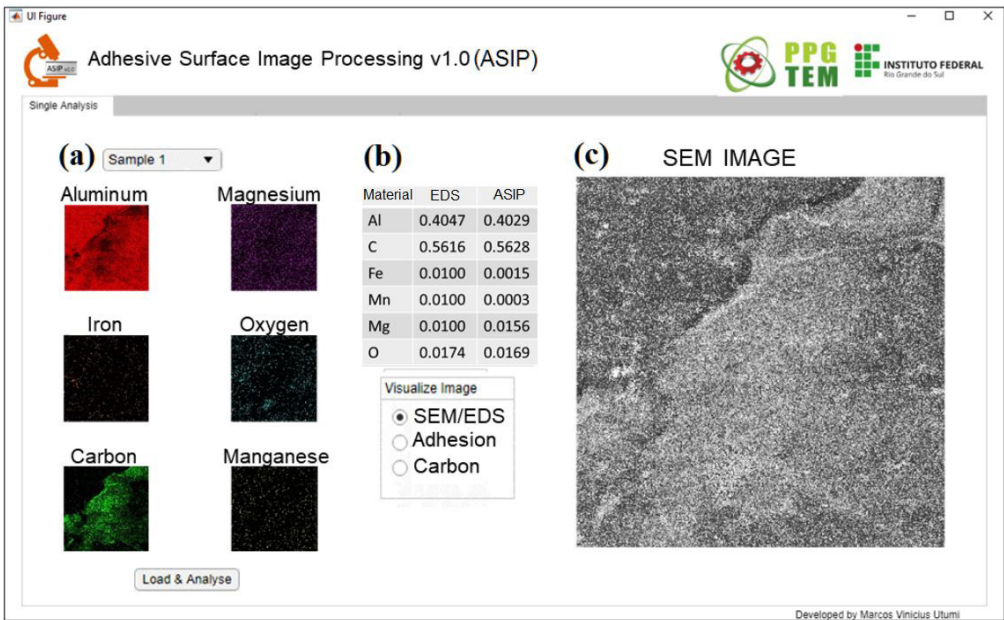


Figure 3. Results screen: a) EDS images; b) Composition of elements (EDS) and image analysis (ASIP); c) SEM image of gross surface being analyzed.

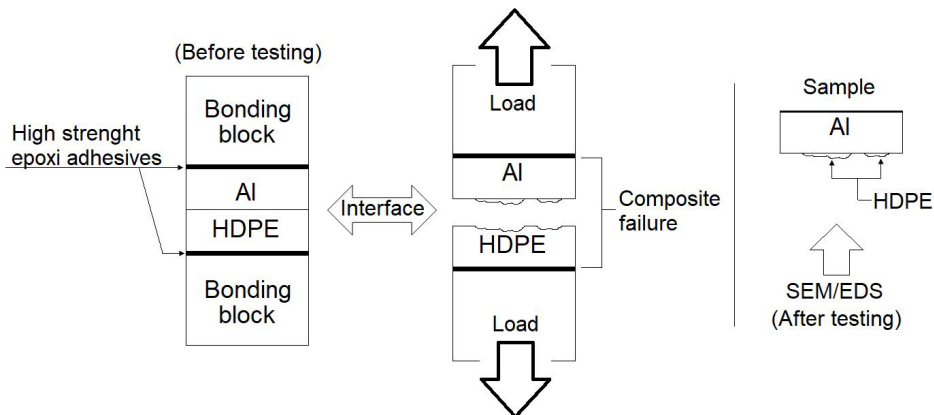


Figure 4. Pull-off test, interfacial fracture of Al/HDPE composite and the sample surface to SEM analysis.

related to the carbon atoms. The processing results in a new image, as seen in Figure 5, where the areas in black represent the cohesive failure, the gray area represents a mixture of both failures and the area in white shows the adhesive failure. The differentiation of the failures is determined visually through the color variation and quantitatively through the chemical composition via EDS on the area analyzed.

In the test sequence, the separate surfaces were analyzed and classified in areas of cohesive and adhesive failures for application in the Equations 7 and 8, where “ σ_z^{flu} ” is the total tensile strength, “ σ_{adh}^{flu} ” is the maximum adhesive failure stress, and “ σ_{coh}^{flu} ” is the maximum cohesive failure stress. The maximum tensile strength equals “ P_{max} ”, maximum load, divided by the total area in Equation 8. “ P_{max} ” is the sum of “ P_{adh} ” and “ P_{coh} ”, adhesive and cohesive forces respectively, as per Equation 9.

$$\sigma_z^{flu} = \sigma_{adh}^{flu} + \sigma_{coh}^{flu} \tag{7}$$

$$\sigma_z^{flu} = \frac{P_{adh}}{Adh_{failure}} + \frac{P_{coh}}{Coh_{failure}} \tag{8}$$

$$P_{max} = P_{adh} + P_{Coh} \tag{9}$$

The method of genetic algorithm (GA) performs directed validations using a set of criteria expressed through conditioning functions^{14,17}. In this study, those functions were applied in multiple analyses to be satisfactory to the results of pull-off tests and, using Equation 8 and the error function, those were the evolution criteria defined in the GA.

It was then possible to quantify the influence of the adhesion and cohesion tests individually, determining the composite interface mechanical properties. The quantification of the stresses influence was carried out through continuous interactions between the populations of adhesion and cohesion stress values in comparison to mechanical tests in relation to a pre-established error. Figure 6 shows the flowchart used for programming the genetic algorithm developed in Matlab[®].

In Figure 7, a pseudo-code of optimization by genetic algorithm implementation represents the GA used in the new method. The algorithm works with an initial population (I) defined in the interface of possible results (n_lim). Through the selection of the population, each individual checked into the functions of mechanical conditions (mech_res). The objective

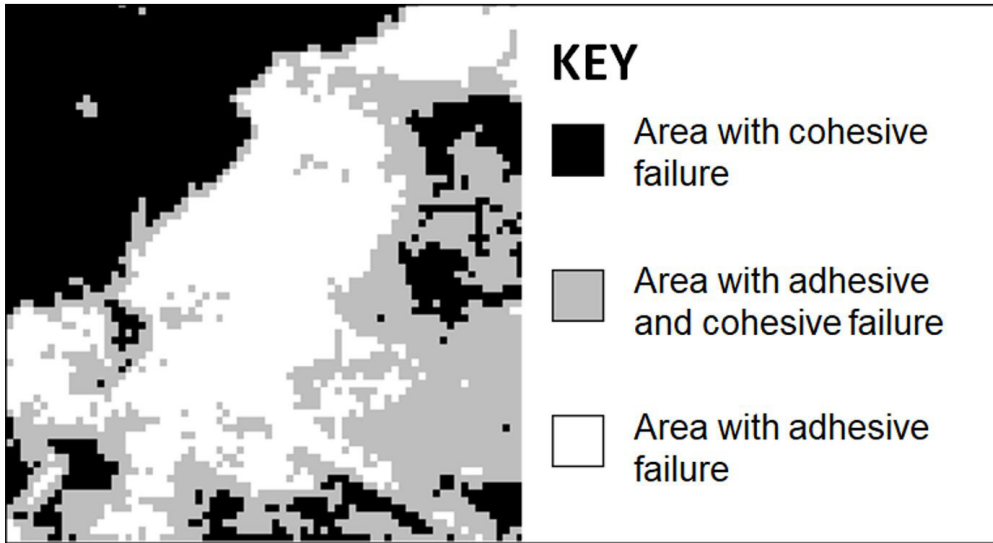


Figure 5. Surface failure analysis, differentiation of adhesive and cohesive failures.

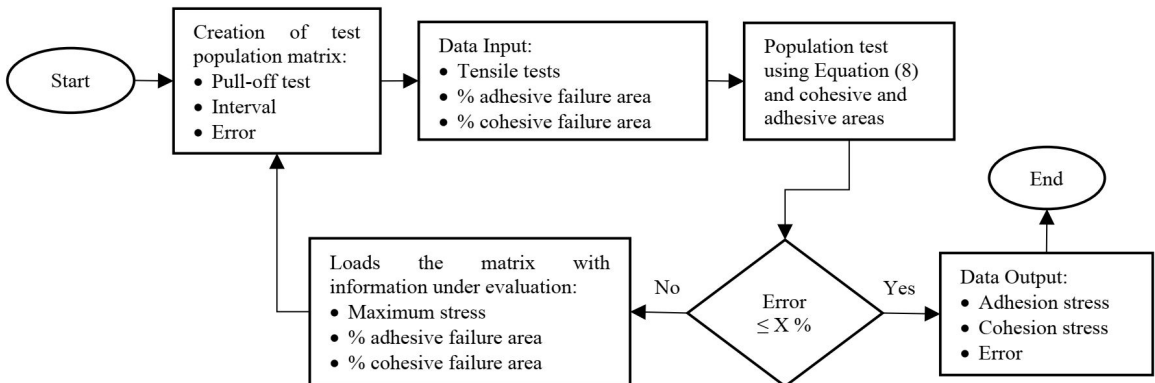


Figure 6. Genetic algorithm flowchart.

function is the attendance of total stress obtained for each sample with the possible value of adhesion and cohesion strengths. After that, a new population is created based on the genetic operators. Each individual tested of each new generation has a relation to the allowed error (allow_error). The stopping criterium only is reached when all individuals have values below the failure limits.

3. Results and Discussion

3.1 Chemical composition evaluation

The application developed resulted in a set of chemical composition values correlated to the digitalized area obtained through SEM/EDS. The maximum error in the equipment results occurred due to the tolerance for the materials with

concentration lower than 1.0%. The average difference between the number obtained through SEM/EDS and the image processing application was lower than 1.0% for all the chemical elements analyzed.

The results of the chemical analysis application are based on the direct relationship between the image generated in the form of a map and the discretization of the spectrogram energy. The image could deliver much more than the surface composition. It also determined and delimited the interface areas – aluminum adhesion and cohesion (bulk) of HDPE. That is due to the aluminum rupture stress being much higher than that of HDPE and also to adhesion in the interface¹⁸.

3.2 Evaluation of the surface and type of failure

Figure 8 presents the two percentages of the total area obtained through the SEM/EDS image analysis. The areas

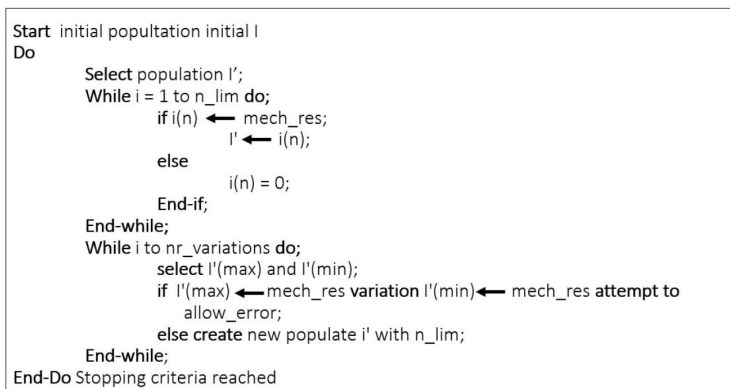


Figure 7. Pseudo code of genetic algorithm implementation.

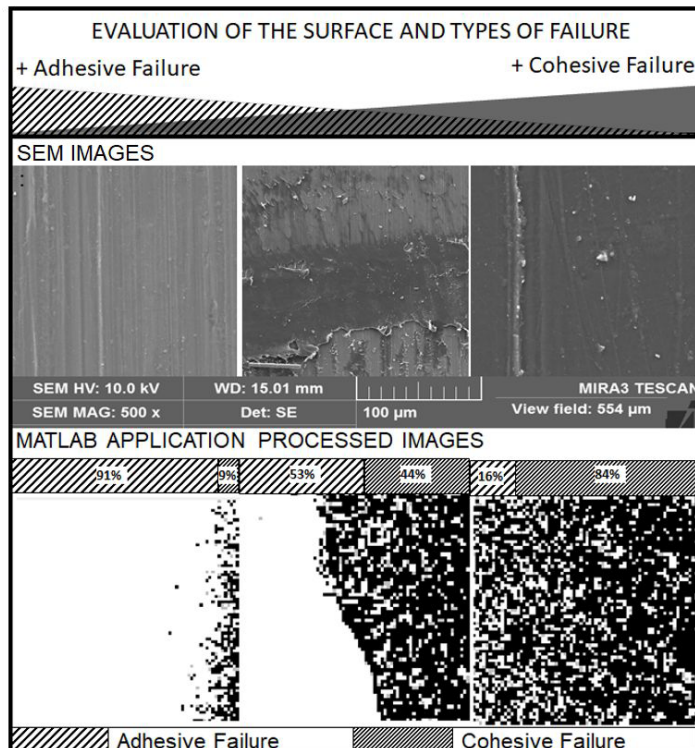


Figure 8. Evaluation of the surface and types of failure.

were organized according to the type of failure. In the images processed by the new method it was possible to identify the cohesive failure through pixels in color black, while the area in white was related to the adhesive failure. Quantitatively, by counting the pixels present in the image using Equations 1, 2 and 3, it was possible to identify a higher presence of carbon for the predominant cohesion failure to the right (84%), whereas it was found that 91% of the total area to the left presented adhesive failure (9% cohesive).

3.3 Mechanical evaluation

Table 1 presents the results obtained according to the ASTM C297¹⁵. The maximum load during the tests was used to determine the maximum stress in the tensile tests, considering a cross section area of 625 mm² for each sample. Table 1 maximum stress values were used in the genetic algorithm evolution programming criteria. Considering the study by Hussein *et al.* in composites made of PE and aluminum sheets using hot pressing, the maximum shear force was up to 2,800.00 N, where a ductile fracture was observed, predominant in the polymer¹⁸. The maximum tensile strength value seen on Table 1, which is 2,242.56 N, also presented the maximum stress with the larger cohesive failure area. Samples 1, 2 and 3 are correlated to the areas in Figure 6, from left to right respectively.

The multiple image analyses and failure areas met the tensile strength results of Table 2, once the different samples with different mechanical results and percentage of failures converge to identical contributions to cohesive and adhesive failures. Besides, for the result obtained using the new method, some PE and aluminum composite references and tests showed a great variability of results in the adhesion tests performed according to previous methods^{18,19}. The numbers

Table 1. Tensile tests results.

Sample	Maximum load (N)	Tensile strength (MPa)
1	555.19	0.89
2	1,399.55	2.24
3	2,242.56	3.59

Table 2. Tensile strengths obtained through image processing and the reference strengths.

Sample	Result	Method
Cohesion Strength: Al/HDPE	4.17 MPa ± 0.001	Tensile strength with image processing in Matlab [®]
Adhesion Strength: Al/HDPE	0.57 MPa ± 0.005	
Al/HDPE: no treatment	1.86 MPa	Double shear test (19)
Al/PE: PE surface treated with acetone	10.9 MPa	Shear stress test ²⁰ (ASTM D1002)

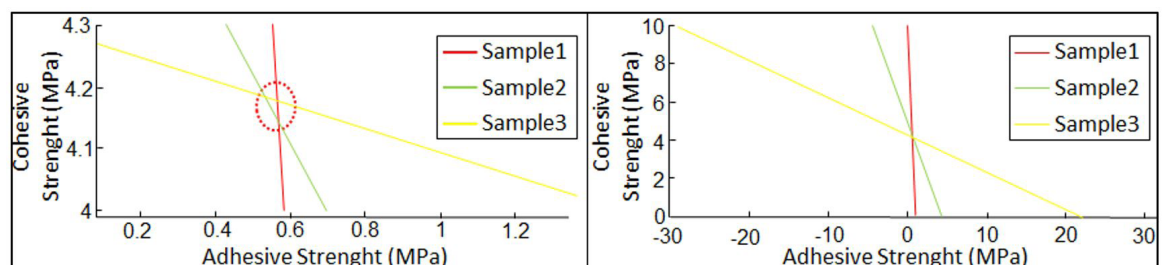


Figure 9. Graphical representation of the convergence region, with predetermined error and refinement, respectively.

obtained depend on several factors, but it is important to correlate the failure areas (Figure 6) with maximum loads to define where the weak point in the structural composite is.

The results obtained through the multiple analysis of images presented on Table 2 can also be observed in Figure 9. The population values of the genetic algorithm are presented in the graphs. In the first graph of Figure 9 left side, there is a dashed circle in red indicating the programmed error convergence area, the three lines represent the specimen's stresses before convergence. The graph on the right side of Figure 9 indicates the convergence into a point that satisfies all the specimens' data. The result obtained considers a margin of error so as to meet a value where the pull-off test data is taken into consideration, if there were more specimens the convergence criteria will absorb these results to obtain the convergence point.

The pure HDPE tensile strength presents a higher value than any other result found in previous studies for Al/HDPE composites¹⁸⁻²⁰. Those results suggest that even in a predominantly cohesive failure, as occurred in sample 3, the maximum stress applied to separate PE from aluminum is still smaller than the resistance to rupture the organic area of the polymer alone.

Previous studies presented a shear resistance of 1.86 MPa and, applying surface treatments to aluminum and polyethylene surfaces, the results were higher than 10.9 MPa²¹. In this study, however, although there was an improvement in the shear resistance with the acetone treatment, there was not a differentiation on the shear adhesive or cohesive stress.

The shear strength and the tensile strength are proportional by a factor of 0.577 using the von Mises equivalent stress equation, considering isotropic and homogeneous materials²². If there is a correlation between these stresses, it is possible to assert that the order of magnitude for pull-off tensile stress found in this study is within the results found in the double shearing¹⁹, as shown on Table 2.

In this study, the mixed adhesion and cohesion stresses was experientially proven by the results of the Al/HDPE tensile tests and, through the application of genetic algorithms in the SEM/EDS analyses, those stresses were distinguished. The

use of the genetic algorithm to optimize mechanical properties had already been applied in the modeling of materials such as steel²³ and sandwich composites¹⁴, as well as the image analyses using SEM to analyze the areas with mechanical failures such as in fatigue cracks²⁴. The combination of those techniques was implemented in this study, allowing for a new approach in the composite materials interface design.

4. Conclusions

The application developed was able to approximate the quantity of each element in the image generated by the SEM/EDS analysis and to calculate the relation between the carbon layer in the delamination area and the type of failure. As expected, as per the images results, the adhesive failure contributed less for the total stress. In pull-off tests for the composite tensile strength, the adhesive area varied from 16% up to 91%, and the maximum stress up to rupture from 0.89 up to 3.59 MPa. The maximum stress found in adhesive failure was 0.57 MPa and for the cohesive failure it was 4.17 MPa, using the GA. The results obtained in this study showed that the SEM/EDS images can also be used in the quantitative evaluation in the distribution of the adhesive and cohesive failure areas and to its effective distinction. After the distribution and quantitative evaluation, the correlation with the mechanical stress results was effective through the genetic algorithm created. The validation is due to the comparison between the areas and the mechanical results, that is, all the samples must be evaluated regarding the type of failure, percentage of area and the pull-off test stress values. The application proved to be a relevant tool to understand the adhesion phenomenon. There was a new approach to use SEM/EDS to evaluate the areas and stresses of failure sites to apply in the metal/polymer composites manufacture and design processes. It also proved to be a robust method since the genetic algorithm developed meets the minimum point through the convergence criteria. However, the analyses require to verify the achievement of these criteria. Some suggestions for future work can similarly apply to the reliability-based design optimization. In this way, the model can present the optimal point and the value of the reliability at the same time.

5. Acknowledgements

The authors are grateful for the support they received from the institutions: Marcopolo S/A, a Brazilian company, and Instituto Federal de Educação, Ciência e Tecnologia do Rio Grande do Sul, a federal education and research institution of Brazil, for the execution of this project.

6. References

1. Utumi MV, Gasparin AL. Desenvolvimento de Material Compósito Sanduíche de Metal/Polímero para Carroceria de Ônibus. In: 23º Congresso Brasileiro de Engenharia e Ciência dos Materiais – CBECIMAT; 2018 Nov 4-8; Foz do Iguaçu, PR. Proceedings. São Paulo: Metallum Congressos Técnicos e Científicos; 2018.
2. Golander C-GG, Sultan B-AA. Surface modification of polyethylene to improve its adhesion to aluminum. *J Adhes Sci Technol.* 1988;2(2):125-35.
3. Khanam PN, AlMaadeed MAA. Processing and characterization of polyethylene-based composites. *Adv Manuf Polym Compos Sci.* 2015;1(2):63-79.
4. Fares O, AL-Oqla FM, Hayajneh MT. Dielectric relaxation of mediterranean lignocellulosic fibers for sustainable functional biomaterials. *Mater Chem Phys.* 2019;229:174-82.
5. Khakpour H, Ayatollahi MR, Akhavan-Safar A, da Silva LFM. Mechanical properties of structural adhesives enhanced with natural date palm tree fibers: effects of length, density and fiber type. *Compos Struct.* 2020;237:111950. <http://dx.doi.org/10.1016/j.compstruct.2020.111950>.
6. AL-Oqla FM, El-Shekeil YA. Investigating and predicting the performance deteriorations and trends of polyurethane bio-composites for more realistic sustainable design possibilities. *J Clean Prod.* 2019;222:865-70.
7. Hirai S, Ishimoto S, Obuchi H, Yao S. Improving the adhesion of polyethylene surfaces using Side-Chain crystalline block copolymer. *J Adhes Sci Technol.* 2019;33(23):2567-78.
8. Algellai AA, Vuksanović MM, Tomić NZ, Marinković AD, Obradović-Đuričić KD, Radojević VJ, et al. The implementation of image analysis for the visualization of adhesion assessment of a composite film. *Mater Lett.* 2018;227:25-8.
9. Jabbari E, Peppas NA. Polymer-polymer interdiffusion and adhesion. *J Macromol Sci Part C.* 1994;34(2):205-41.
10. Baszkin A, Ter-Minassian-Saraga L. Effect of surface polarity on self-adhesion of polymers. *Polymer (Guildf).* 1978;19(9):1083-8.
11. Gong L, Xiang L, Zhang J, Chen J, Zeng H. Fundamentals and advances in the adhesion of polymer surfaces and thin films. *Langmuir.* 2019;35(48):15914-36.
12. Gasparin AL, Wanke CH, Nunes RCR, Tentardini EK, Figueroa CA, Baumvol IJR, et al. An experimental method for the determination of metal-polymer adhesion. *Thin Solid Films.* 2013;534:356-62.
13. Füllbrandt M, Kesal D, Klitzing R v. Work of adhesion between metals and polymers on a macro- and microscopic scale. In: 16th European Conference on Composite Materials, ECCM 2014; 2014 Jun 22-26; Seville, Spain. Proceedings. Patras, Greece: ESCM; 2014.
14. Canyurt OE, Meran C, Uslu M. Strength estimation of adhesively bonded tongue and groove joint of thick composite sandwich structures using genetic algorithm approach. *Int J Adhes Adhes.* 2010;30(5):281-7. <http://dx.doi.org/10.1016/j.ijadhadh.2009.09.005>.
15. ASTM International. ASTM C297/C297M-16 AI: Standard test method for flatwise tensile strength of sandwich constructions. West Conshohocken, PA: ASTM 2016.
16. Toygar ME, Tee KF, Maleki FK, Balaban AC. Experimental, analytical and numerical study of mechanical properties and fracture energy for composite sandwich beams. *J Sandw Struct Mater.* 2019;21(3):1167-89.
17. Garshasbi NIAN, Eskandari JAMJ, Garshasbinia N, Jam JE. Identification of mechanical properties in laminated composite plates using genetic algorithm. *Iran Polym J.* 2005;14(1):39-46.
18. Hussein SK, Mhessan AN, Alwan MA. Hot press joining optimization of Polyethylene to Aluminium Alloy AA6061-T6 Lap joint using design of experiments. *Eng J (NY).* 2017;21(7):157-69.
19. Morris CEMM. Adhesive bonding of polyethylene. *J Appl Polym Sci.* 1970;14(9):2171-81.
20. Harold S, Schouhorn H, Proviencence N. Bonding technique. *J Am Soc Nav Eng.* 1965;39(4):620-2.
21. Landgrebe D, Müller R, Haase R, Scholz P, Riemer M, Albert A, et al. Efficient Manufacturing Methods for Hybrid Metal-Polymer Components. In: ASME 2016 International Mechanical Engineering Congress and Exposition; 2016 Nov 11-17; Phoenix, Arizona. Proceedings. Nova Iorque: American Society of Mechanical Engineers; 2016. p. V002T02A053-V002T02A053.

22. Ahn HS, Roylance BJ. Stress behaviour of surface-coated materials in concentrated sliding contact. *Surf Coatings Technol* [Internet]. 1990 Feb [cited 2020 Apr 7];41(1):1–15. Available from: <https://www.sciencedirect.com/science/article/abs/pii/025789729090126W>
23. Nath A, Ray KK, Barai SV. Evaluation of ratcheting behaviour in cyclically stable steels through use of a combined kinematic-isotropic hardening rule and a genetic algorithm optimization technique. *Int J Mech Sci*. 2018;2019(152):138-50. <http://dx.doi.org/10.1016/j.ijmecsci.2018.12.047>.
24. Reid A, Marshall M, Kabra S, Minniti T, Kockelmann W, Connolley T, et al. Application of neutron imaging to detect and quantify fatigue cracking. *Int J Mech Sci*. 2019;159(May):182-94. <http://dx.doi.org/10.1016/j.ijmecsci.2019.05.037>.